Molecular Crystals and Liquid Crystals

ISSN: 1542-1406 (Print) 1563-5287 (Online) Journal homepage: http://www.tandfonline.com/loi/gmcl20

Protonic Transport Analysis of Starch-Chitosan Blend Based Electrolytes and Application in Electrochemical Device

M. F. Shukur, R. Ithnin & M. F. Z. Kadir

To cite this article: M. F. Shukur, R. Ithnin & M. F. Z. Kadir (2014) Protonic Transport Analysis of Starch-Chitosan Blend Based Electrolytes and Application in Electrochemical Device, Molecular Crystals and Liquid Crystals, 603:1, 52-65, DOI: 10.1080/15421406.2014.966259

To link to this article: http://dx.doi.org/10.1080/15421406.2014.966259

Published online: 15 Dec 2014.

Submit your article to this journal

Article views: 51

View related articles

View Crossmark data

Full Terms & Conditions of access and use can be found at
http://www.tandfonline.com/action/journalInformation?journalCode=gmcl20

Download by: [University Town Library of Shenzhen] **Date:** 02 January 2016, At: 00:40

Mol. Cryst. Liq. Cryst., Vol. 603: pp. 52–65, 2014
Copyright © Taylor & Francis Group, LLC
ISSN: 1542-1406 print/1563-5287 online
DOI: 10.1080/15421406.2014.966259

Taylor & Francis
Taylor & Francis Group

Protonic Transport Analysis of Starch-Chitosan Blend Based Electrolytes and Application in Electrochemical Device

M. F. SHUKUR,[1] R. ITHNIN,[2] AND M. F. Z. KADIR[2,*]

[1]Institute of Graduate Studies, University of Malaya, 50603, Kuala Lumpur, Malaysia
[2]Centre for Foundation Studies in Science, University of Malaya, 50603, Kuala Lumpur, Malaysia

Two polymer electrolyte systems (unplasticized and plasticized) based on starch-chitosan blend doped with ammonium bromide (NH_4Br) were prepared. The conductivity was found to be influenced by the number density (n) and mobility (μ) of the ions. The highest conducting plasticized electrolyte had n and μ values of 8.75×10^{18} cm^{-3} and 1.03×10^{-3} cm^2 V^{-1} s^{-1}, respectively. Ionic transference number for the highest conducting plasticized electrolyte was found to be 0.92. An electrochemical double layer capacitor (EDLC) using the highest conducting plasticized electrolyte was cycled for 500 times at 0.048 mA cm^{-2}.

Keywords Polymer electrolyte; starch-chitosan blend; ammonium bromide; transference number; EDLC

1. Introduction

Electrochemical devices such as batteries, solar cells, fuel cells, and electrochemical double layer capacitors (EDLCs) are constantly being investigated for energy storage [1–8]. The device performance depends strongly on the electrolyte employed [9–13]. Liquid electrolytes are preferred to be used in electrochemical devices due to their high ionic conductivity [14, 15]. However, the use of a liquid electrolyte in electrochemical devices suffers from problems, e.g. leakage, corrosion and solvent evaporation at high temperature [16–18]. Hence, researchers have turned their attention to solid polymer electrolytes (SPEs) which offer advantages such as thermally stable, the ability to eliminate corrosive solvents and harmful gas formation, and low volatility with easy handling [19]. However, the conductivity obtained by SPEs still needs to be improved.

The polymer blending method has been reported to be able to increase the conductivity of electrolytes [20–22]. According to Buraidah and Arof [21], blending two polymers can provide more complexation sites at which ion hopping and exchange can take place leading to an increase in conductivity. The conductivity of starch-ammonium nitrate (NH_4NO_3)

*Address correspondence to M. F. Z. Kadir, Centre for Foundation Studies in Science, University of Malaya, 50603 Kuala Lumpur, Malaysia. Tel.: +60379675916; Fax: +60379676478. E-mail: mfzkadir@um.edu.my

Color versions of one or more of the figures in the article can be found online at www.tandfonline.com/gmcl.

Downloaded by [University Town Library of Shenzhen] at 00:40 02 January 2016

Downloaded by [University Town Library of Shenzhen] at 00:40 02 January 2016

increased from 2.83 $\times$ 10^{-5} S cm^{-1} to 3.89 $\times$ 10^{-5} S cm^{-1} by using a starch–chitosan blend [23, 24]. From our previous works, the conductivity of chitosan-ammonium bromide (NH_4Br) increased from (4.38 $\pm$ 1.26) $\times$ 10^{-7} S cm^{-1} to (9.72 $\pm$ 0.95) $\times$ 10^{-5} S cm^{-1} when using a starch-chitosan blend as the polymer host [25, 26]. The blend of starch and chitosan was reported to form mechanically stable films due to the inter- and intra-molecular hydrogen bonding that formed between the hydroxyl and amino groups of starch and chitosan [27]. Plasticization is another approach to enhance the conductivity of the electrolyte. According to Ismail et al. [28], the addition of plasticizer can soften the polymer backbone, enabling the coordination sites to become closer to each other. Hence, the ions require less energy to hop over to the next site. The plasticization method also can dissociate more salt to become ions which contributes towards ionic conduction [29]. The conductivity of $\sim 10^{-7}$ S cm^{-1} of a chitosan–lithium acetate (LiOAc) electrolyte was increased to 5.5 $\times$ 10^{-6} S cm^{-1} when plasticized with palmitic acid [30, 31]. The addition of ethylene carbonate (EC) to chitosan-ammonium iodide (NH_4I) increased the conductivity from 3.7 $\times$ 10^{-7} S cm^{-1} to 7.6 $\times$ 10^{-6} S cm^{-1} [32]. In this work, EC was chosen as plasticizer since its dielectric constant value ($\varepsilon_{EC} = 89$) is high compared to other plasticizers such as propylene carbonate (PC) ($\varepsilon_{PC} = 64$) and dimethyl phthalate (DMP) ($\varepsilon_{DMP} = 8.5$). The transport analysis of unplasticized and plasticized starch-chitosan blend based electrolytes doped with NH_4Br is reported and the highest conducting plasticized electrolyte is used in the fabrication of an electrochemical double layer capacitor (EDLC).

2. Experimental

For preparation of an unplasticized system, 0.8 g starch (Brown and Polson) was dissolved in 100 ml of 1% acetic acid (SYSTERM) at 80°C for 20 min. After the solution cooled to room temperature, 0.2 g chitosan [viscosity: 800–2000 cP, 1 wt% in 1% acetic acid (25°C), Sigma-Aldrich] was added. Different amounts of NH_4Br (Bendosen) were added and stirred until homogenous solutions were obtained. For preparation of a plasticized system, different amounts of EC (Merck) were added to the highest conducting unplasticized electrolyte solutions. All homogenous solutions were cast on plastic Petri dishes and left to dry at room temperature. The dry films were kept in a desiccator filled with silica gel dessicants for further drying.

X-ray diffraction (XRD) measurements were carried out on a Siemens D5000 X-ray diffractometer where X-rays of 1.5406 Å wavelengths were generated by a Cu Kα source. The 2θ angle was varied from 5° to 80° at a resolution of 0.1°. The degree of crystallinity (χ_c) of the electrolytes was calculated using:

$$\chi_c = \frac{A_c}{A_T} \times 100\% \tag{1}$$

where A_c and A_T are the areas of crystalline and total hump, respectively. The areas of crystalline and total hump were determined using OriginPro8 software.

The conductivity (σ) of the electrolytes was calculated using:

$$\sigma = \frac{d}{R_b A} \tag{2}$$

where d is the thickness of the electrolyte, R_b is bulk resistance and A is the electrode- electrolyte contact area. The value of R_b was determined from the Cole-Cole plot obtained from

impedance measurements of the electrolytes. The electrolytes were sandwiched between two stainless steel electrodes of a conductivity holder. The impedance measurements were conducted using HIOKI 3532-50 LCR HiTESTER from room temperature to 348 K in the frequency range of 50 Hz to 5 MHz.

The ionic transference number was measured using Wagner's DC polarization method [33]. The cell consisted of the highest conducting plasticized electrolyte sandwiched by two stainless steel (SS) blocking electrodes (SS/SPE/SS), which was polarized using a V&A Instrument DP3003 digital DC power supply at 0.80 V. The DC current was monitored as a function of time. The measurement was undertaken at room temperature.

The electrochemical stability window of the highest conducting plasticized electrolyte was studied using linear sweep voltammetry (LSV). The LSV measurement was performed using a Digi-IVY DY2300 potentiostat at a scan rate of 5 mV s^{-1} at room temperature. The highest conducting electrolyte was sandwiched between two stainless steel electrodes, where one of the electrodes was used as the working electrode while the other one was used as counter and reference electrodes. The voltage range is from 0 to 2.4 V.

For the preparation of the EDLC electrode, 13 g activated carbon (RP20, manufactured by Kuraray, Japan), 2 g polyvinylidene fluoride (PVdF) and 1 g carbon black (Super P) were mixed together in 60 ml of N-methyl pyrrolidone (NMP) (EMPLURA) and stirred until homogenous. The mixture was doctor-bladed on an aluminum foil and heated at 60°C for drying. The dried electrode was kept in a desiccator containing silica gel. Cyclic voltammetry (CV) of the EDLC at room temperature was carried out using a Digi-IVY DY2300 potentiostat from 0 to 0.85 V at various scan rates. The charge-discharge characteristics of the EDLC were performed using a Neware battery cycler at a constant current density of 0.048 mA cm^{-2} for 500 cycles. The discharge capacitance (C) of the EDLC was calculated using

$$C = \frac{i}{m}\left(\frac{1}{s}\right) \tag{3}$$

where i is the constant current, m is mass of active material and s is the slope of the discharge curve. The specific capacity (Q) was evaluated using Eq. (4), where t_d is the discharge time.

$$Q = \frac{t_d i}{m} \tag{4}$$

3. Results and Discussion

From the XRD study by Zhai et al. [34], the blend of 80 wt% corn starch and 20 wt% chitosan was the most amorphous and the blend exhibited a better tensile strength than the other blend ratios. Since the amorphous structure is an important criterion for ionic conduction, in the present work, the blend of 80 wt% starch and 20 wt% chitosan was chosen to host the protonic conduction. The addition of salt to the polymer host is expected to increase the amorphous phase of the electrolyte. The X-ray diffractogram of selected electrolytes in unplasticized system is shown in Fig. 1(a). From our previous work [26], the room temperature conductivity of the electrolyte increases as NH_4Br content increases to 35 wt%. This result is evidenced by the value of χ_c as shown in Table 1. The percentage of the crystalline phase decreased when NH_4Br content increased up to 35 wt%. As the ion concentration in the electrolyte increased, both the fraction of amorphous phase and charge carriers increased simultaneously [35]. It was reported that ions are favorably mobile in

Downloaded by [University Town Library of Shenzhen] at 00:40 02 January 2016

Downloaded by [University Town Library of Shenzhen] at 00:40 02 January 2016

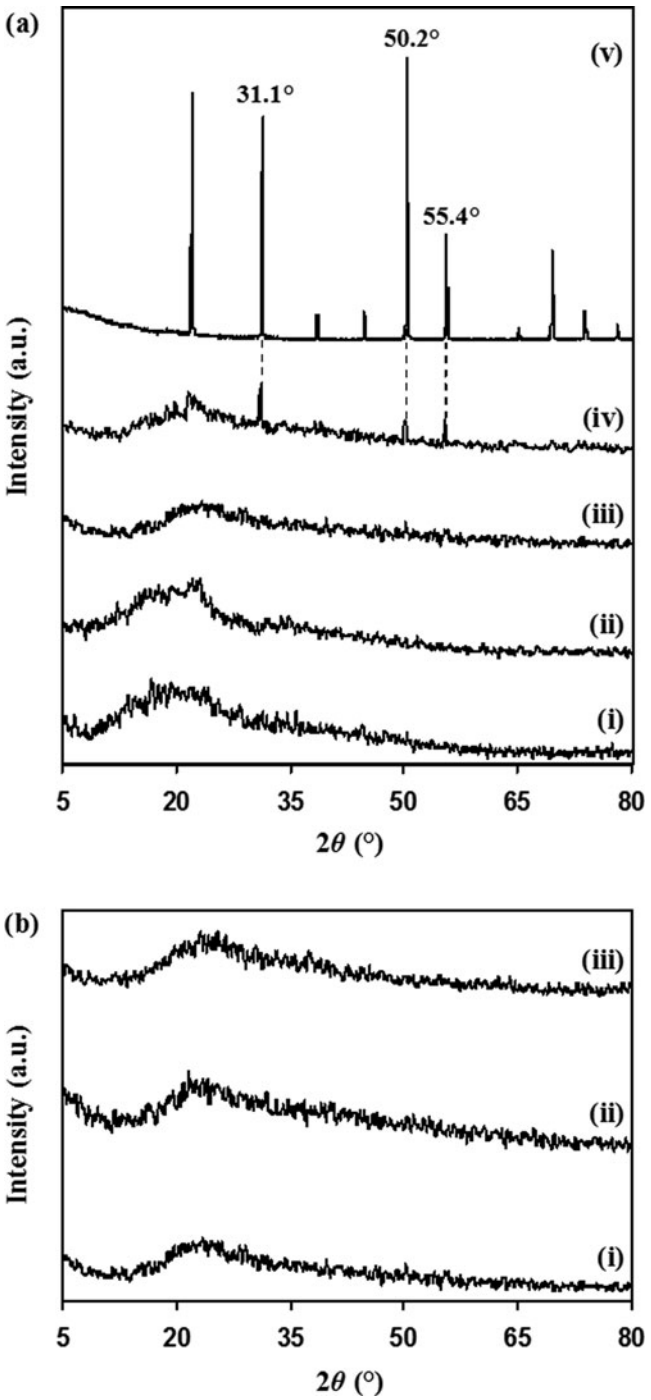

Figure 1. (a) X-ray diffractogram of pure starch-chitosan blend film (i), starch-chitosan blend with 5 wt% NH_4Br (ii), 35 wt% NH_4B4 (iii), 45 wt% NH_4Br (iv) electrolytes, and pure NH_4Br salt powder (v). (b) X-ray diffractogram of unplasticized starch-chitosan-NH_4Br (i), starch-chitosan-NH_4Br with 10 wt% EC (ii), and 30 wt% EC (iii) electrolytes.

Table 1. Degree of crystallinity of selected electrolytes in unplasticized system

Sample (wt% NH_4Br)	χ_c (%)
5	37.40
35	30.70
45	35.90

the amorphous phase since their motion is assisted by polymer segmental motion [36–38]. The XRD results explain the increasing conductivity value with increasing NH_4Br content up to 35 wt%. The room temperature conductivity decreases with addition of more than 35 wt% NH_4Br [26]. From the X-ray diffractogram of the electrolyte with 45 wt% NH_4Br in Fig. 1(a) (iv), three crystalline peaks appear at 31.1°, 50.2°, and 55.4°. These three peaks are the characteristic peaks of NH_4Br salt as shown in Fig. 1(a) (v). From Table 1, the χ_c value of the electrolyte with 45 wt% NH_4Br was higher than the electrolyte with 35 wt% NH_4Br. This result shows that the ions have recrystallized on addition of 45 wt% NH_4Br, leading to a decrease in conductivity. The conductivity enhancement due to plasticization can also be explained by the XRD patterns as shown in Fig. 1(b). From a previous report [26], the addition of 30 wt% EC increases the conductivity to $(1.44 \pm 0.51) \times 10^{-3}$ S cm^{-1}. The addition of EC as a plasticizer promotes ion dissociation [39]. This is because the plasticizer has a high dielectric constant that can weaken the Coulombic force between the anion and cation of the salt so that the salt can be easily dissociated, thus increasing the ion concentration and the amorphous phase within the electrolyte [40]. From Table 2, the χ_c value decreases as EC content increases to 30 wt%. This result verifies the conductivity result as reported previously [26].

The influence of temperature on conductivity is depicted in Fig. 2. The conductivity of all electrolytes increased linearly with increasing temperature, hence obeying the Arrhenius rule. Therefore, there is neither a phase transition in the polymer matrix nor a domain formed by the addition of salt [41]. The Arrhenian conductivity–temperature relationship has been observed for starch-NH_4NO_3 [23], chitosan-NH_4I [32] and polyvinyl alcohol (PVA)-NH_4Br [42] electrolytes. The activation energy (E_a) of each electrolyte is calculated from the following Arrhenius equation:

$$\sigma = \sigma_o \exp\left[-\frac{E_a}{kT}\right] \tag{5}$$

where σ_o is the pre-exponential factor, k is the Boltzmann constant and T is the absolute temperature. The value of E_a for each unplasticized and plasticized electrolyte is tabulated in

Table 2. Degree of crystallinity of selected electrolytes in plasticized system

Sample (wt% EC)	χ_c (%)
0	30.70
10	28.02
30	26.63

Downloaded by [University Town Library of Shenzhen] at 00:40 02 January 2016

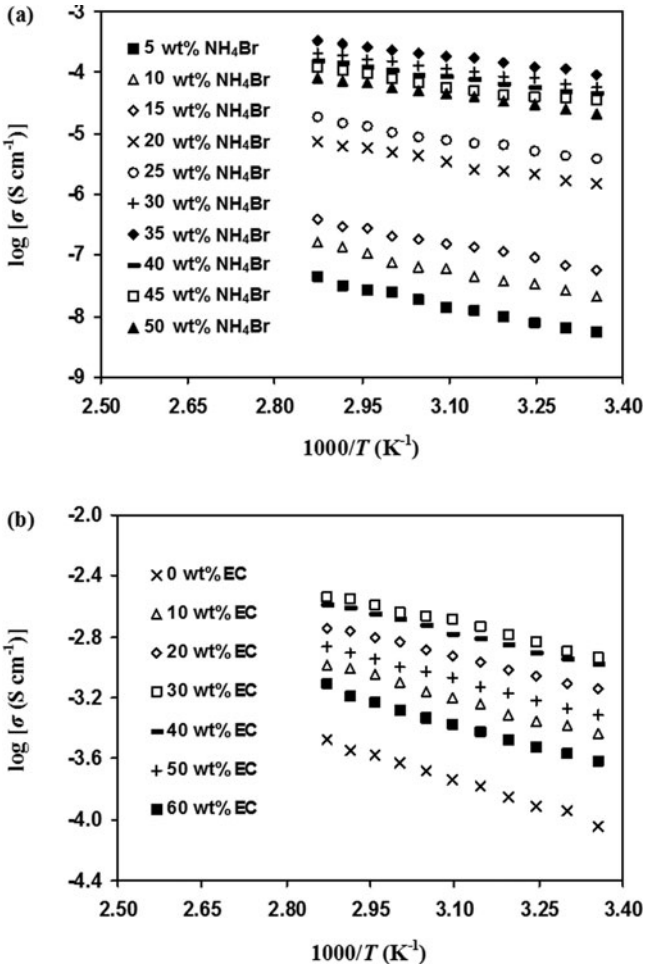

Figure 2. Variation of conductivity as a function of temperature for unplasticized system (a) and plasticized system (b).

Tables 3 and 4, respectively. The value of E_a was found to be 0.22–0.37 eV for unplasticized electrolytes and 0.17–0.20 eV for plasticized electrolytes. The higher conducting electrolyte had the lower E_a value. This is in agreement with the fact that the conductivity increases with the increase in number density of ions as shown in Tables 3 and 4. Thus the energy barrier for the proton transport decreases leading to a decrease in the E_a value [43].

Transport parameters of each electrolyte were obtained using Rice and Roth model [44]. In this model, conductivity can be expressed as:

$$\sigma = \frac{2}{3}\left[\frac{(Ze)^2}{kTm}\right] n E_a \tau \exp\left(\frac{-E_a}{kT}\right) \tag{6}$$

where Z is the valency of conducting species, e is electron charge, m is mass of the charge carrier, n is number density of ions and τ is the traveling time of ions. The value of τ was

Downloaded by [University Town Library of Shenzhen] at 00:40 02 January 2016

Table 3. Transport parameters of each electrolyte in unplasticized system at room temperature

Sample (wt% NH_4Br)	σ (S cm^{-1})	E_a (eV)	τ (s)	n (cm^{-3})	μ (cm^2 V^{-1} s^{-1})
5	$(4.53 \pm 1.61) \times 10^{-9}$	0.37	1.24×10^{-13}	4.49×10^{16}	6.28×10^{-7}
10	$(1.30 \pm 0.38) \times 10^{-8}$	0.36	1.25×10^{-13}	8.87×10^{16}	9.15×10^{-7}
15	$(6.83 \pm 0.41) \times 10^{-7}$	0.33	1.31×10^{-13}	1.51×10^{17}	2.82×10^{-6}
20	$(1.71 \pm 0.25) \times 10^{-6}$	0.29	1.42×10^{-13}	5.87×10^{17}	1.82×10^{-5}
25	$(3.52 \pm 0.35) \times 10^{-6}$	0.27	1.45×10^{-13}	8.33×10^{17}	2.64×10^{-5}
30	$(5.59 \pm 0.81) \times 10^{-5}$	0.23	1.57×10^{-13}	3.02×10^{18}	1.16×10^{-4}
35	$(9.72 \pm 0.95) \times 10^{-5}$	0.22	1.60×10^{-13}	3.64×10^{18}	1.67×10^{-4}
40	$(5.54 \pm 0.99) \times 10^{-5}$	0.23	1.57×10^{-13}	2.99×10^{18}	1.16×10^{-4}
45	$(3.43 \pm 0.89) \times 10^{-5}$	0.24	1.53×10^{-13}	2.68×10^{18}	7.99×10^{-5}
50	$(2.58 \pm 0.42) \times 10^{-5}$	0.24	1.53×10^{-13}	2.01×10^{18}	7.99×10^{-5}

obtained using the equation:

$$\tau = \frac{l}{v} \tag{7}$$

where l is the jump distance between two complexation sites. In this work, l is the distance between two repeating units of amylose fiber in starch, which is 10.4 Å [23]. The velocity (v) of mobile ions was obtained using:

$$v = \sqrt{\frac{2E_a}{m}} \tag{8}$$

The ionic mobility, μ was calculated using the value of n.

$$\mu = \frac{\sigma}{ne} \tag{9}$$

The transport parameters for unplasticized and plasticized electrolytes are tabulated in Tables 3 and 4, respectively. The values of n and μ increased with increasing conductivity. For the unplastcized system, the highest conducting electrolyte with incorporation of 35 wt% NH_4Br had the highest n and μ values of 3.64×10^{18} cm^{-3} and 1.67×10^{-4} cm^2

Table 4. Transport parameters of each electrolyte in plasticized system at room temperature

Sample (wt% EC)	σ (S cm^{-1})	E_a (eV)	τ (s)	n (cm^{-3})	μ (cm^2 V^{-1} s^{-1})
10	$(3.93 \pm 0.85) \times 10^{-4}$	0.19	1.72×10^{-13}	4.92×10^{18}	4.98×10^{-4}
20	$(9.58 \pm 2.26) \times 10^{-4}$	0.17	1.82×10^{-13}	5.82×10^{18}	1.03×10^{-3}
30	$(1.44 \pm 0.51) \times 10^{-3}$	0.17	1.82×10^{-13}	8.75×10^{18}	1.03×10^{-3}
40	$(1.08 \pm 0.15) \times 10^{-3}$	0.17	1.82×10^{-13}	6.56×10^{18}	1.03×10^{-3}
50	$(4.03 \pm 1.20) \times 10^{-4}$	0.19	1.72×10^{-13}	5.05×10^{18}	4.98×10^{-4}
60	$(2.06 \pm 0.53) \times 10^{-4}$	0.20	1.68×10^{-13}	3.71×10^{18}	3.46×10^{-4}

Downloaded by [University Town Library of Shenzhen] at 00:40 02 January 2016

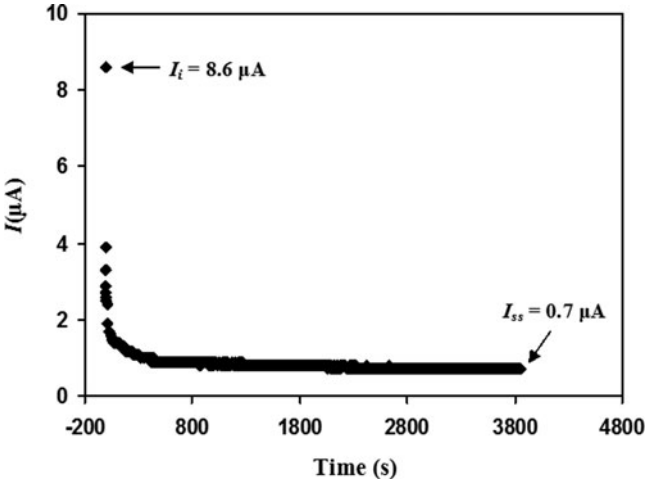

Figure 3. Transference number of the highest conducting electrolyte in plasticized system at room temperature using stainless steel electrodes.

V^{-1} s^{-1}, respectively. The values of n and μ for the highest conducting chitosan-NH_4Br electrolyte were 4.81×10^{17} cm^{-3} and 5.69×10^{-6} cm^2 V^{-1} s^{-1}, respectively [25]. It is known that blending two polymers can provide more complexation sites at which ion hopping and exchange can take place [21]. For starch-chitosan blend, hydrogen bonding interactions occurred between the hydroxyl groups of starch and the amino groups of chitosan [26, 45]. This hydrogen bonding interaction created more complexation sites for ions to transport [46]. This phenomenon increases the number density and mobility of ions. For the plasticized system, the highest conducting electrolyte with incorporation of 30 wt% EC had the highest n and μ values of 8.75×10^{18} cm^{-3} and 1.03×10^{-3} cm^2 V^{-1} s^{-1}, respectively. Other reports also show that the increasing conductivity of the electrolyte is influenced by the increase in n and μ values [23, 39, 47–50].

The contribution of ions to the total conductivity of an electrolyte can be determined from the transference number measurement [51]. From the plot of polarization current against time in Fig. 3, the transference numbers of ion (t_{ion}) and electron (t_e) for the highest conducting plasticized electrolyte were calculated using:

$$t_{ion} = \frac{I_i - I_{ss}}{I_i} \tag{10}$$

$$t_e = \frac{I_{ss}}{I_i} \tag{11}$$

where I_i is the initial current and I_{ss} is the steady state current. The steady state is achieved when the movement of mobile ions is balanced by diffusion process, which is due to the ion concentration gradient [52]. The concentration gradient is ascribed to the non unity transference number of ions in the polymer electrolyte, which cause a decay in current to a lower steady state value [53]. It was found that t_{ion} was 0.92 and t_e was 0.08, indicating that the charge transport in the polymer complex is predominantly due to ions. Hema et al. [54] reported that t_{ion} for all the compositions of the PVA-NH_4Br electrolyte systems lies between 0.93 and 0.96 at 303 K. The ionic transference number for potato starch-ammonium

Downloaded by [University Town Library of Shenzhen] at 00:40 02 January 2016

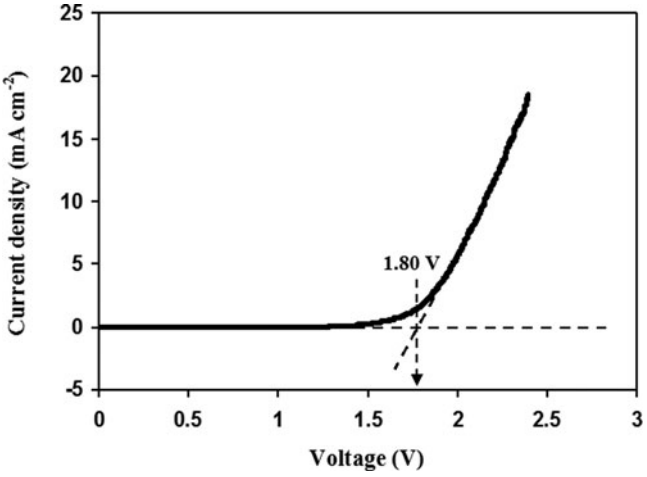

Figure 4. Linear sweep voltammogram of the highest conducting electrolyte in plasticized system at 5 mV s^{-1}.

iodide (NH_4I) electrolyte was reported to be >0.95 [55]. Aziz *et al.* [56] showed that t_{ion} for the highest conducting phthaloyl chitosan-ammonium thiocyanate (NH_4SCN) electrolyte was 0.912. The results from the literature are comparable with the present work.

LSV measurement was carried out in order to determine the stability window of the electrolyte as well as the maximum operational voltage of an electrochemical device employing the electrolyte [40]. From the literature, there are many reports on studies of the electrochemical stability of proton conducting polymer electrolytes using stainless steel working, counter and reference electrodes [56–60]. In the present work, the linear sweep voltammogram is shown in Fig. 4. It can be observed that the decomposition voltage of the

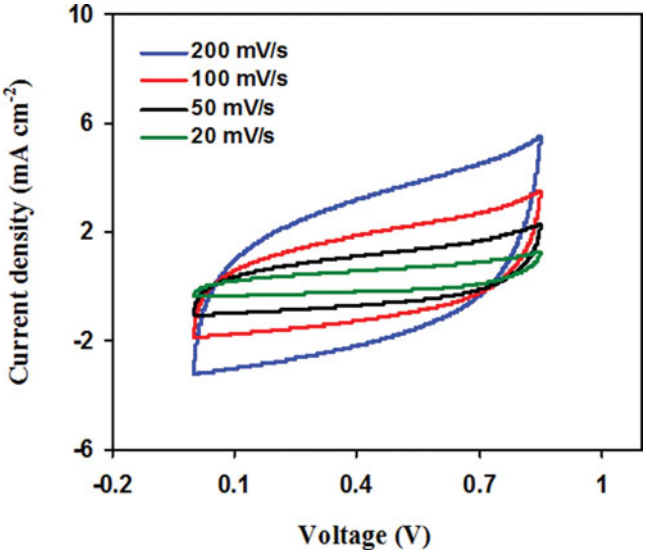

Figure 5. Cyclic voltammogram of EDLC at different scan rates.

Downloaded by [University Town Library of Shenzhen] at 00:40 02 January 2016

Downloaded by [University Town Library of Shenzhen] at 00:40 02 January 2016

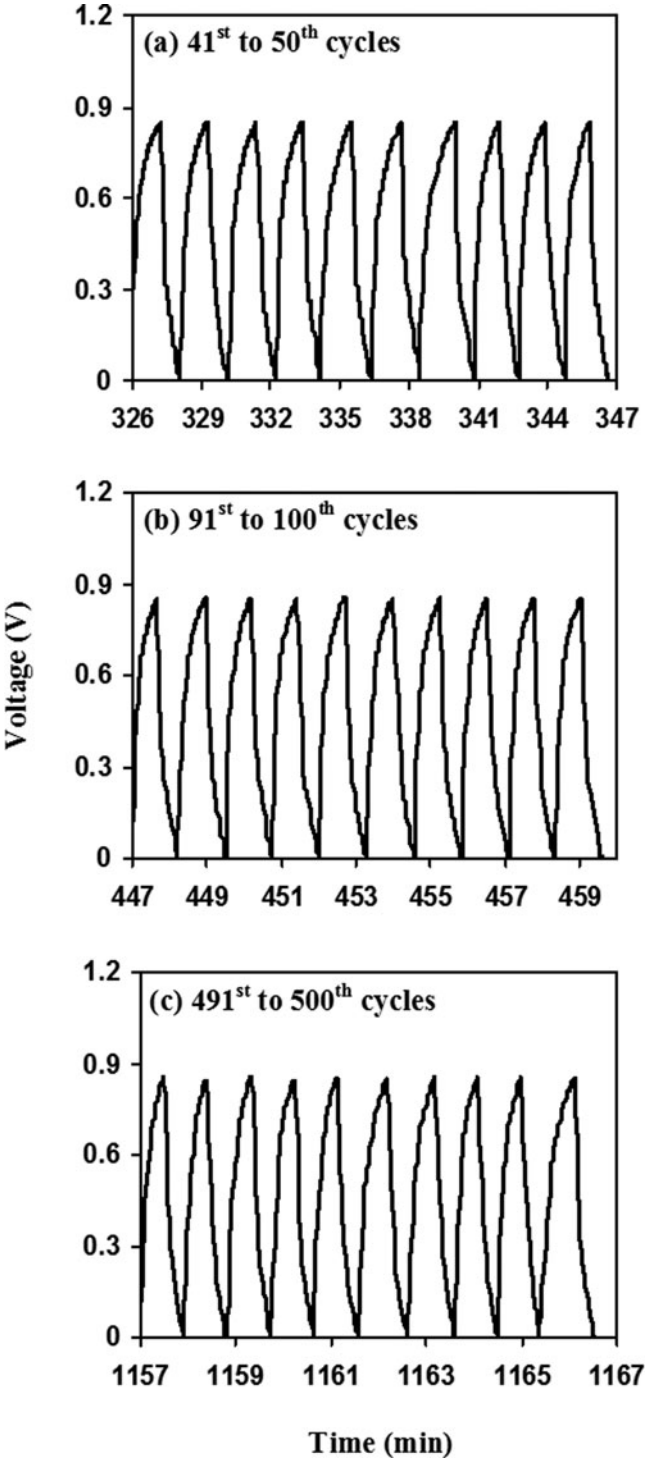

Figure 6. Charge-discharge curves of the EDLC at selected cycles.

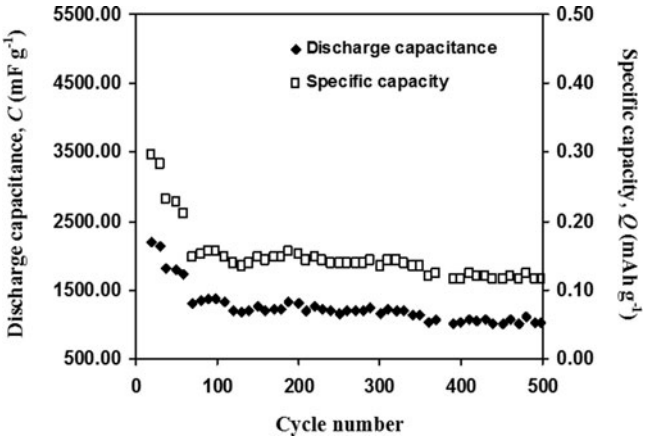

Figure 7. Discharge capacitance and specific capacity versus cycle number.

highest conducting electrolyte in the plasticized system was 1.80 V. The breakdown voltage of chitosan-NH_4NO_3-EC electrolyte with stainless steel working, counter and reference electrodes was reported to be 1.80 V [57], which is comparable with our result. According to Pratap et al. [61], the standard electrochemical window of proton batteries is $\sim$ 1 V. Arof et al. [51] reported that the decomposition voltage of polymethyl methacrylate (PMMA)-lithium bis(oxalate borate) (LiBOB) electrolyte with stainless steel working, counter and reference electrodes is 1.7 V and the electrolyte was used in the fabrication of EDLC. The present result shows that the highest conducting electrolyte in the present work is suitable for fabrication of an electrochemical device.

The cyclic voltammograms of the EDLC were recorded in the potential range of 0–0.85 V at different scan rates as shown in Fig. 5. The voltammograms of the EDLC at 20 and 50 mV s^{-1} exhibited almost ideal horizontal plateaus inferring ion diffusion occurred at fairly constant rate with little impact from ohmic resistance [51]. As the scan rate increased to 100 and 200 mV s^{-1}, the discrepancy from a perfect rectangular shape for the cyclic voltammogram can be assigned to the internal resistance and the carbon porosity, which produced a current dependence of the potential [62]. Since the fabricated EDLC is scan rate dependent, it can be concluded that the EDLC showed the characteristic of a capacitor cell [63]. From the voltammogram, it can be inferred that charge and discharge of the fabricated EDLC was almost reversible at the electrode/electrolyte interface [64].

The cycle life performance is important for practical applications. Figure 6 shows the typical charging and discharging performance of the EDLC at a constant current density of 0.048 mA cm^{-2} between 0 to 0.85 V for selected cycles. In the present work, the EDLC charge-discharge curves were quite comparable to those reported in the literature [40, 41, 65, 66]. Using the slope of the discharge curves, the values of C were calculated using Eq. (3) and are shown in Fig. 7. Towards the 70th cycle, the value of C was observed to decrease to 1306 mF g^{-1}. After the 70th cycle, the value of C remained constant at $\sim$ 1172 mF g^{-1} until it completed 500 cycles. Shuhaimi et al. [66] reported that the value of C of the EDLC using methyl cellulose (MC)-NH_4NO_3 electrolyte was 1.67 F g^{-1} (1670 mF g^{-1}) at the 15th cycle. According to Arof et al. [51], the C value of activated carbon AC/PMMA-LiBOB/AC EDLC remains constant for almost 50 cycles at $\sim$ 500 mF g^{-1}. The Q value of the present EDLC, calculated using Eq. (4), was also decreasing to 0.1484 mAh g^{-1} towards the 70th cycle and remained constant at $\sim$ 0.1400 mAh g^{-1} until it completed

Downloaded by [University Town Library of Shenzhen] at 00:40 02 January 2016

500 cycles. For the first 70 cycles, the decrease in C and Q values might be due to the depletion of the polymer electrolyte, as the number of charge carriers within the polymer was reduced with increasing cycle number [60].

4. Conclusions

Starch-chitosan blend based electrolytes doped with NH_4Br and plasticized with EC were prepared and characterized. From the XRD measurements, the electrolyte with 35 wt% NH_4Br is the most amorphous electrolyte in an unplasticized system, while the electrolyte with 30 wt% EC was the most amorphous electrolyte in the plasticized system. This result verifies our room temperature conductivity result from previous work. The conductivity-temperature relationship for all electrolytes is Arrhenian. The number density and mobility of ions for the highest conducting electrolyte in the unplasticized system were 3.64×10^{18} cm^{-3} and 1.67×10^{-4} cm^2 V^{-1} s^{-1}, respectively. The highest conducting electrolyte in the plasticized system had a number density and mobility of ions of 8.75×10^{18} cm^{-3} and 1.03×10^{-3} cm^2 V^{-1} s^{-1}, respectively. The ionic transference number of the highest conducting plasticized electrolyte was 0.92. LSV analysis shows that the highest conducting plasticized electrolyte is suitable for EDLC application. The fabricated EDLC has been cycled for 500 times. The discharge capacitance and specific capacity of the EDLC at the 500th cycle were $\sim$ 1172 mF g^{-1} and $\sim$ 0.1400 mAh g^{-1}, respectively.

Downloaded by [University Town Library of Shenzhen] at 00:40 02 January 2016

Funding

The authors thank the University of Malaya for the RP010A-13AFR grant provided.

References

[1] Shuhaimi, N. E. A., Alias, N. A., Kufian, M. Z., & Arof, A. K. (2012). *J. Solid State Electrochem.*, *14*, 2153.
[2] Wei, Y.-Z., Fang, B., Iwasa, S., & Kumagai, M. (2005). *J. Power Sources*, *141*, 386.
[3] Chen, Z., Lu, W. Q., Liu, J., & Amine, K. (2006). *Electrochim. Acta*, *51*, 3322.
[4] Kufian, M. Z., Aziz, M. F., Shukur, M. F., Rahim, A. S., Ariffin, N. E., Shuhaimi, N. E. A., Majid, S. R., Yahya, R., & Arof, A. K. (2012). *Solid State Ionics*, *208*, 36.
[5] Buraidah, M. H., Teo, L. P., Majid, S. R., & Arof, A. K. (2010). *Opt. Mater.*, *32*, 723.
[6] Ito, S., Hirata, T., Mori, D., Benten, H., Ohkita, H., & Honda, S. (2012). *Mol. Cryst. Liq. Cryst.*, *578*, 19.
[7] Thomberg, T., Janes, A., & Lust, E. (2010). *Electrochim. Acta*, *55*, 3138.
[8] Morni, N. M., & Arof, A. K. (1999). *J. Power Sources.*, *77*, 42.
[9] Hofmann, A., Schulz, M., & Hanemann, T. (2013). *Electrochim. Acta*, *89*, 823.
[10] Takami, N., Sekino, M., Ohsaki, T., Kanda, M., & Yamamoto, M. (2001). *J. Power Sources*, *97–98*, 677.
[11] McBreen, J., Lee, H. S., Yang, X. Q., & Sun, X. (2000). *J. Power Sources*, *89*, 163.
[12] Park, M., Zhang, X., Chung, M., Less, G. B., & Sastry, A. M. (2010). *J. Power Sources*, *195*, 7904.
[13] Rao, M., Geng, X., Liao, Y., Hu, S., & Li, W. (2012). *J. Membr. Sci.*, *399-400*, 37.
[14] Perera, K., & Dissanayake, M. A. K. L. (2006). *Sri Lankan J. Phys.*, *7*, 1.
[15] Deepa, M., Sharma, N., Agnihotry, S. A., Singh, S., Lal, T., & Chandra, R. (2002). *Solid State Ionics*, *152-153*, 253.
[16] Lee, C.-P., Chen, P.-Y., Vittal, R., & Ho, K.-C. (2010). *J. Mater. Chem.*, *20*, 2356.
[17] Lee, C.-P., Lin, L.-Y., Chen, P.-Y., Vittal, R., & Ho, K.-C. (2010) *J. Mater. Chem.*, *20*, 3619.
[18] Chen, P.-Y., Lee, C.-P., Vittal, R., & Ho, K.-C. (2010). *J. Power Sources*, *195*, 3933.

[19] S. Ramesh, S., Liew, C.-W., & Arof, A. K. (2011). *J. Non-Cryst. Solids*, *357*, 3654.
[20] Baskaran, R., Selvasekarapandian, S., Kuwata, N., Kawamura, J., & Hattori, T. (2006). *Solid State Ionics*, *177*, 2679.
[21] Buraidah, M. H., & Arof, A. K. (2011). *J. Non-Cryst. Solids*, *357*, 3261.
[22] Choi, N. S., & Park, J. K. (2001). *Electrochim. Acta*, *46*, 1453.
[23] Khiar, A. S. A., & Arof, A. K. (2010). *Ionics*, *16*, 123.
[24] Khiar, A. S. A., & Arof, A. K. (2011). *World Acad. Sci. Eng. Technol.*, *59*, 23.
[25] Shukur, M. F., Azmi, M. S., Zawawi, S. M. M., Majid, N. A., Illias, H. A., & Kadir, M. F. Z. (2013). *Phys. Scr.*, *T157*, 014049.
[26] Shukur, M. F., Majid, N. A., Ithnin, R., & Kadir, M. F. Z. (2013). *Phys. Scr.*, *T157*, 014051.
[27] Lu, D. R., Xiao, C. M., & Xu, S. J. (2009). *Express Polym. Lett.*, *3*, 366.
[28] Ismail, L., Majid, S. R., & Arof, A. K. (2011). *Mater. Res. Innov.*, *13*, 282.
[29] Shukur, M. F., Yusof, Y. M., Zawawi, S. M. M., Illias, H., & Kadir M. F. Z. (2013). *Phys. Scr.*, *T157*, 014050.
[30] Yahya, M. Z. A., & Arof, A. K. (2002). *Eur. Polym. J.*, *38*, 1191.
[31] Yahya, M. Z. A., & Arof, A. K. (2003). *Eur. Polym. J.*, *39*, 897.
[32] Buraidah, M. H., Teo, L. P., Majid, S. R., & Arof, A. K. (2009). *Physica B*, *404*, 1373.
[33] Wagner, J. B., & Wagner, C. J. (1957). *J. Chem. Phys.*, *26*, 1597.
[34] Zhai, M., Zhao, L., Yoshii, F., & Kume, T. (2004). *Carbohydr. Polym.*, *57*, 83.
[35] Aji, M. P., Masturi, Bijaksana, S., Khairurrijal, & Abdullah, M. (2012). *Am. J. Appl. Sci.*, *9*, 946.
[36] Li, G., Li, Z., Zhang, P., Zhang, H., & Wu, Y. (2008). *Pure Appl. Chem.*, *80*, 2553.
[37] Noda, A., & Watanabe, M. (2000). *Electrochim. Acta*, *45*, 1265.
[38] Xu, W., Belieres, J. P., & Angell, C. A. (2001). *Chem. Mater.*, *13*, 575.
[39] Kadir, M. F. Z, Majid, S. R., & Arof, A. K. (2010). *Electrochim. Acta*, *55*, 1475.
[40] Arof, A. K., Shuhaimi, N. E. A., Alias, N. A., Kufian, M. Z., & Majid, S. R. (2010). *J. Solid State Electrochem.*, *14*, 2145.
[41] Sudhakar, Y. N., & Selvakumar, M. (2012). *Electrochim. Acta*, *78*, 398.
[42] Hema, M., Selvasekarapandian, S., Arunkumar, D., Sakunthala, A., & Nithya, H. (2009). *J. Non-Cryst. Solids*, *355*, 84.
[43] Selvasekarapandian, S., Baskaran, R., & Hema, M. (2005). *Physica B*, *357*, 412.
[44] Rice, M. J., & Roth, W. L. (1972). *J. Solid State Chem.*, *4*, 294.
[45] Salleh, E., Muhamad, I. I., & Khairuddin, N. (2009). *World Acad. Sci. Eng. Technol.*, *3*, 403.
[46] Shukur, M. F., Ithnin, R., Illias, H., & Kadir, M. F. Z. (2013). *Opt. Mater.*, *35*, 1834.
[47] Samsudin, A. S., Khairul, W. M., & Isa, M. I. N. (2012). *J. Non-Cryst. Solids*, *358*, 1104.
[48] Majid, S. R., & Arof, A. K. (2005). *Physica B*, *355*, 78.
[49] Winie, T., & Arof, A. K. (2006). *Ionics*, *12*, 149.
[50] Winie, T., Ramesh, S., & Arof, A. K. (2009). *Physica B*, *404*, 4308.
[51] Arof, A. K., Kufian, M. Z., Syukur, M. F., Aziz, M. F., Abdelrahman, A. E., & Majid, S. R. (2012). *Electrochim. Acta*, *74*, 39.
[52] Woo, H. J., Majid, S. R., & Arof, A. K. (2011). *Mater. Res. Innov.*, *15*, 49.
[53] Bhargav, P. B., Mohan, V. M., Sharma, A. K., & Rao, V. V. R. N. (2009). *Curr. Appl. Phys.*, *9*, 165.
[54] Hema, M., Selvasekerapandian, S., Sakunthala, A., Arunkumar, D., & Nithya, H. (2008). *Physica B*, *403*, 2740.
[55] Kumar, M., Tiwari, T., & Srivastava, N. (2012). *Carbohydr. Polym.*, *88*, 54.
[56] Aziz, N. A., Majid, S. R., & Arof, A. K. (2012). *J. Non-Cryst. Solids*, *358*, 1581.
[57] Ng, L. S., & Mohamad, A. A. (2008). *J. Membr. Sci.*, *325*, 653.
[58] Shuhaimi, N. E. A., Teo, L. P., Woo, H. J., Majid, S. R., & Arof, A. K. (2012). *Polym. Bull.*, *69*, 807.
[59] Samsudin, A. S., Lai, H. M., & Isa, M. I. N. (2014). *Electrochim. Acta*, *129*, 1.
[60] Liew, C.-W., Ramesh, S., & Arof, A. K. (2013). *Int. J. Hydrogen Energ.*, *39*, 2953.
[61] Pratap, R., Singh, B., & Chandra, S. (2006). *J. Power Sources*, *161*, 702.

Downloaded by [University Town Library of Shenzhen] at 00:40 02 January 2016

[62] Kadir, M. F. Z., Aspanut, Z., Yahya, R. & Arof, A. K. (2011). *Mater. Res. Innov.*, *15*, S164.
[63] Hashmi, S. A., Kumar, A., & Tripathi, S. K. (2007). *J. Phys. D: Appl. Phys.*, *40*, 6527.
[64] Yang, C.-C., Hsu, S.-T., & Chien, W.-C. (2005). *J. Power Sources*, *152*, 303.
[65] Kumar, M. S., & Bhat, D. K. (2009). *Physica B*, *404*, 1143.
[66] Shuhaimi, N. E. A., Majid, S. R., & Arof, A. K. (2009). *Mater. Res. Innov.*, *13*, 239.

Downloaded by [University Town Library of Shenzhen] at 00:40 02 January 2016